The Biophysicist

Barriers to Diffusion in Cells: Visualization of Membraneless Particles in the Nucleus

Leonel Malacrida[1,2,3,§], Per Niklas Hedde[1,§], Belen Torrado[1,4], Enrico Gratton[1,*]

[1]Laboratory for Fluorescence Dynamics, Department of Biomedical Engineering, University of California, Irvine, CA 92697, USA
[2]Unidad de Microscopia Avanzada y Bifotónica, Departamento de Fisiopatología, Hospital de Clínicas, Facultad de Medicina, Universidad de la República, Uruguay
[3]Advanced Bioimaging Unit, Institut Pasteur de Montevideo, Uruguay
[4]Laboratory of Human Molecular Genetics, Institut Pasteur de Montevideo, Uruguay

ABSTRACT Transient barriers are fundamental to cell supramolecular organization and assembly. Discontinuities between spaces can be generated by a physical barrier but also by thermodynamic barriers achieved by phase separation of molecules. However, because of the transient nature and the lack of a visible barrier, the existence of phase separation is difficult to demonstrate experimentally. We describe an approach based on the 2-dimensional pair correlation function (2D-pCF) analysis of the spatial connectivity in a cell. The educational aim of the article is to present both a model suitable for explaining diffusion barrier measurements to a broad range of courses and examples of biological situations. If there are no barriers to diffusion, particles could diffuse equally in all directions. In this situation the pair correlation function introduced in this article is independent of the direction and is uniform in all directions. However, in the presence of obstacles, the shape of the 2D-pCF is distorted to reflect how the obstacle position and orientation change the flow of molecules. In the example shown in this article, measurements of diffusion of enhanced green fluorescent protein moving in live cells show the lack of connectivity at the nucleolus surface for shorter distances. We also observe a gradual increase in the connectivity for longer distances or times, presumably because of molecular trajectories around the nucleolus.

KEY WORDS fluorescence correlation; spectroscopy; fluoroscene workshop; membraneless organelles; connectivity maps

I. INTRODUCTION

This article is intended as a guide for teachers in a course describing the motion of molecules in cells in the presence of obstacles small and large found in the cell. We believe that the subject is important for modelers and to biologists in general. How molecules diffuse in biological systems is necessary for the introduction of the concept of compartments in cells and in tissues. In compartments, biochemical reactions can be accelerated in one compartment and kept separated from other compartments. The corresponding author (EG) has used part of the material of this article in the course BME 138 (Biospectroscopy for Undergraduates) and for the graduate course BME 238 (Biospectroscopy for Graduates). First, we describe the nature of the physical phenomena we intend to address; then we propose

"§" equal contribution

"*" corresponding author

Received: 4 September 2019
Accepted: 4 May 2020
Published: 13 August 2020

Downloaded from http://meridian.allenpress.com/the-biophysicist/article-pdf/1/2/9/2580574/i2578-6970-1-2-9.pdf by guest on 01 October 2020

graphical methods that should be understandable by the general reader. The graphical methods described in this article are the results of classroom experience by one of the authors (EG) who regularly teaches the subject to a relatively large class of senior undergraduate, master's, and graduate students. The style of teaching was changed to graphical illustrations after negative experience using a mathematically rigorous approach.

II. MOVEMENT OF MOLECULES IN THE PRESENCE OF OBSTACLES

In cells, a universal mechanism of transport of molecules to their target location is thermal diffusion. However, in the cell interior, molecules find barriers to diffusion, as well as obstacles they have to go around (1, 2). Diffusion in the presence of obstacles of arbitrary shape and size cannot be described by simple mathematics. The cell interior has large membrane structures such as the nuclear envelope, the Golgi apparatus, and the endoplasmic reticulum, which are different in shape, size, and location in every cell (3, 4). The nucleus contains organelles like the nucleoli and Cajal bodies devoid of a membrane. It is believed that these organelles are segregated by a liquid–liquid phase separation (4–6). In principle, if we could track each molecule, or at least molecules of a given kind, we could produce a map of barriers by observing where the molecules cannot go (7). However, molecules and barriers move much too quickly to track them individually. There are also too many molecules of a given kind in the cell to track individually. Molecules diffuse in a cell with a diffusion constant of about 20 $\mu m^2/s$, and they can diffuse through pores at the nuclear membrane or to the exterior of the cytosol. The diffusion in the cell interior is a 3-dimensional (3D) process, and current methods for single-particle tracking can only explore relatively small volumes in 3D. Averaging methods, such as photobleaching recovery, cannot provide information about the motion of single molecules. New techniques capable of resolving the path followed by single molecules are needed, with enough temporal and spatial resolution to follow fast-diffusing molecules, possibly in a volume as large as the entire nucleus or the entire cell (8–10). The pair correlation algorithm described in this work calculates the time it takes for molecules to go between a pair of points in the cell, hence the name "pair correlation function" (10, 11). To explain our method, we use a graphical representation of the diffusional process starting at an arbitrary point in the cell and measuring the time needed to travel a given distance from that point. The expectation is that if the space is homogeneous, the time to reach a given distance is independent of the specific direction. However, if during the diffusion process a molecule encounters an impenetrable barrier, like the membrane in a cell, that molecule will never reach a point on the other side of the barrier. That is, the pair correlation function calculated for 2 points on opposite sides of an impenetrable barrier will be zero. If instead of an impenetrable barrier there is an obstacle that the molecule must go around, it will take a longer time to get to the point after the obstacle than if the obstacle is absent. These are the elementary concepts that form the basis of the visualization of barriers to diffusion in a cell. A tangible analogy of a barrier to diffusion could be a river or a fence. If a person or animal is on one side of a fence, they will not be found on the other side at any later time, because they cannot cross. Another simple analogy could be that between 2 points there is an obstacle like a mountain. In this case, there is a probability to find the person or animal on the other side of the mountain, but it will take longer to get there compared with traveling the same distance in the absence of the obstacle. We can extend the concept by considering how barriers might affect the probability of finding a person or animal that was at one point at a given time to be at a different point at a later time. These concepts should be intuitive to every student.

In fluctuation spectroscopy using a confocal microscope (or a camera), the volume of excitation is diffraction-limited, being about

Downloaded from http://meridian.allenpress.com/the-biophysicist/article-pdf/1/2/9/2580574/i2578-6970-1-2-9.pdf by guest on 01 October 2020

0.2 femtoliters. This volume contains (depending on the concentration of the fluorescent proteins) about 1–100 molecules. The average fluorescence (due mainly to nonmoving molecules) is subtracted from the fluorescence (the average value) in the correlation function, leaving only the correlations due to the moving fluorescent particles. The fluorescence signals appear as single events because of single moving particles. The field of fluorescence correlation spectroscopy (FCS) in a single point was originally developed in 1973 by Magde *et al*. (12). Today, most of the experiments are done with images, but the pixel size is diffraction-limited and the number of moving molecules in a pixel is low. This is a well-understood principle in FCS and among the community working on single-molecule fluctuations. What is new here is the cross-correlation between the fluctuations at a pair of distant points originating from the same molecule as it diffuses in a cell. In the following part of this article we describe the consequences of these basic principles, and we focus on the visualization of obstacles to diffusion in cells, but the concepts apply to the macroscopic world as well. In the macroscopic world you could take a picture, but in the cells you could take a picture only if you are able to label the barrier; otherwise, one can infer the existence of an invisible barrier because molecules cannot pass through. However, to describe the physical process we are trying to model, we are adding the mathematical expressions of the 2-dimensional pair correlation function (2D-pCF), which is the cross-correlation of fluorescence fluctuations at 2 distant points in a cell or tissue (10). The pair correlation function is defined in Eq. 1.

$$\mathrm{pCF}(\tau, \delta r) = \frac{< F(t,0)F(t+\tau, \delta r)}{\langle F(t,0)\rangle \langle F(t,\delta r)\rangle} \qquad (1)$$

The pCF is indexed by 2 variables, δr and τ. The time τ is the usual variable indicating the time delay between the records of fluorescence intensity fluctuations at 2 different points separated by a distance δr. In this article we will use units of pixels to indicate the distance. Of course, we need to specify the size of a pixel. The pCF is defined next, for which the angle brackets ($\langle\ \rangle$) indicate the sum over all possible times in the record, and F indicates the fluorescence intensity at time τ and position δr after the average is subtracted. For an introduction to fluorescence, consult the book *Introduction to Fluorescence* by D.M. Jameson (13).

III. A GRAPHICAL REPRESENTATION OF THE PRINCIPLE OF PAIR CORRELATION FUNCTIONS

In this article we make an effort to describe the process of detecting barriers to diffusion without using the mathematical formula (Eq. 1) given in section II in hopes of explaining the visualization of barrier to diffusion to the nonexpert in spatial correlation methods. The pair correlation formula (2D-pCF) calculates the cross-correlation between fluorescence fluctuations at different points in a cell (10, 11). Fluorescence is used as a means to observe the fluctuations due to moving molecules. The basic idea is that fluctuations in fluorescence intensity are caused by the movement of single molecules through a pixel or volume of excitation. By correlating the fluctuations at a given distance between pairs of points, we can obtain the probability for a molecule (the same molecule) to go from one point to another and the time it takes for this displacement to occur. If this concept becomes difficult for the audience, the example of people or animals moving in the presence of obstacles could work as well.

A typical pCF is shown in Figure 1A. This function increases first to reach a maximum and then decreases later to zero, which simply means there is a maximum probability to find the molecule, person, or animal at a given distance and a given time. In the case of random motion, the probability is minimal at short times (because it has not reached a given distance) and tends to zero at very long times because the object has gone too far. In the 2D-pCF approach we calculate the pCF starting at one pixel (r_0), for all pixels in the image at a given distance R from the original pixel in the

Downloaded from http://meridian.allenpress.com/the-biophysicist/article-pdf/1/2/9/2580574/i2578-6970-1-2-9.pdf by guest on 01 October 2020

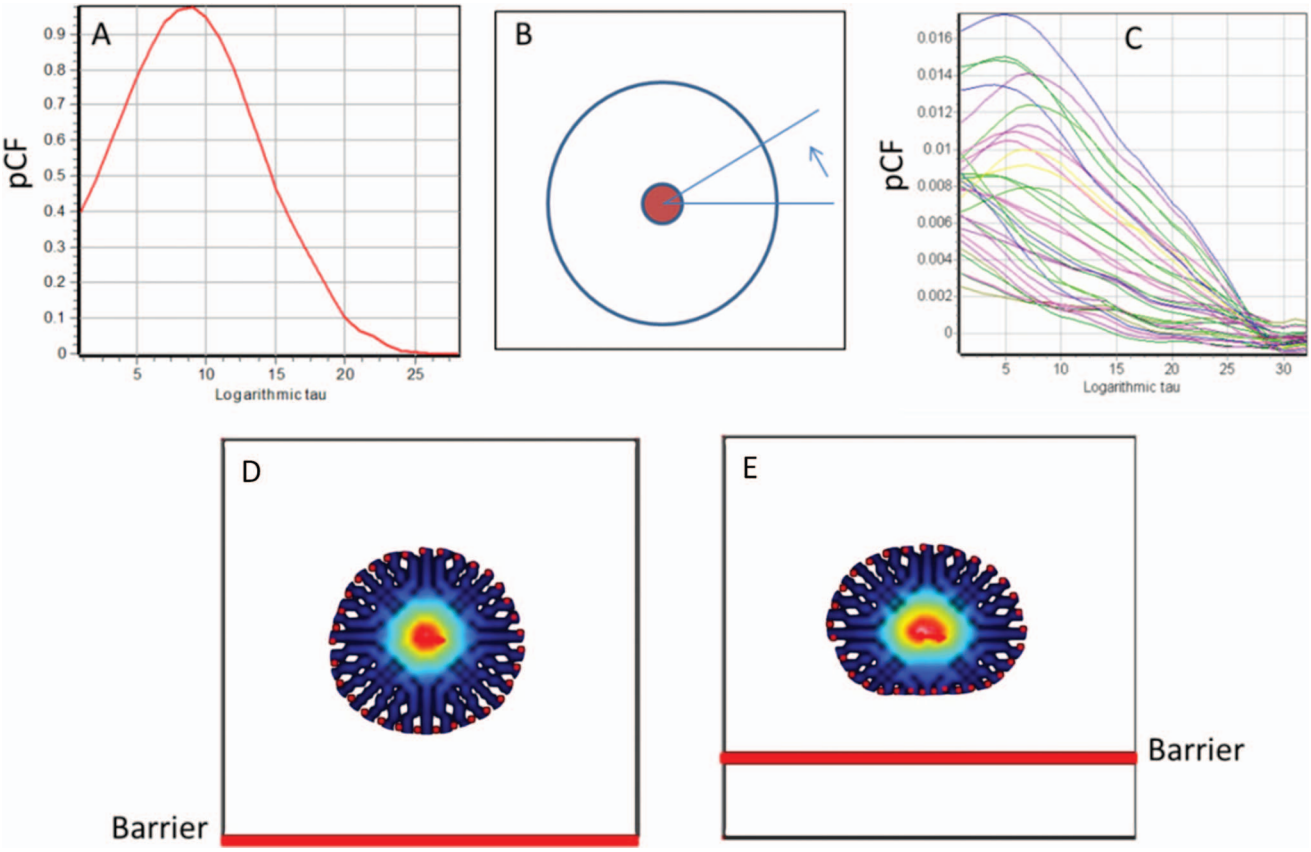

Fig 1. (A) A typical pair correlation function. Note that this correlation function could have a maximum. (B) The algorithm calculates the correlation (Eq. 1) at a number of angles shown by the arrow with respect to one point in the cell marked in red. (C) At different angles, the correlation function could be different if the diffusion is not isotropic. (D) The set of correlation functions in panel C is plotted in polar coordinates in a figure called the SPRITE for a given point. (E) If there is an obstacle at a given distance, the shape of the SPRITE will be deformed. Note that the deformation of the SPRITE follows the direction of the obstacle. The closer the point is to the obstacle, the larger will be the deformation of the SPRITE.

plane of the image, which means we are looking around in all directions. We calculate the pCF (the probability to find the object in a given direction) at 32 angles equally spaced around a circle (Fig 1B,C). The 2D-pCF(τ, R) is given by the set of pCFs (32 angles in the example in Fig 1) calculated for pixels at a given distance R. The pCFs are also logarithmically averaged with 32 equally log-spaced time intervals. For each pixel of the image, we obtain a subimage (32 $\times$ 32 pixels) organized by the angle and the delay time index (Fig 1D,E). This subimage is then represented in polar coordinates so that the angle of the polar plot corresponds to the angle of the original pCF in the image grid, as shown in Figure 1D. We call this polar plot a SPRITE, which is the 2D-pCF(τ, R) at each point of the image as a function of the angle and plotted on a log time axis, where R is an integer describing the distance in units of pixels between any 2 points in the image. This representation may not be obvious to people not familiar with coordinate systems. In this case, the teacher could ask for students to participate in a real experiment: start to walk in all directions and measure the time it takes to arrive to a given distance or how far the person has traveled for a given amount of time. Although the SPRITE looks like an image (32 $\times$ 32 points), the dimensions of the axes of the SPRITE are in log time units. In Figure 1D,E we show 2 representative SPRITEs away from and close to an impenetrable barrier to diffusion indicated by the red line.

Because each SPRITE is like a small image, we use moment analysis (pattern recognition) to characterize some elements of the angular distribution in the SPRITE. Finally, we define

Downloaded from http://meridian.allenpress.com/the-biophysicist/article-pdf/1/2/9/2580574/i2578-6970-1-2-9.pdf by guest on 01 October 2020

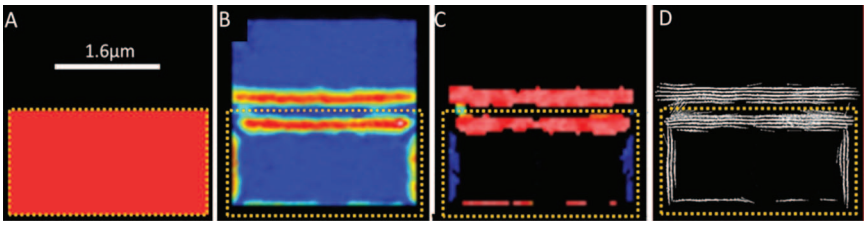

Fig 2. Simulation of fluorescent molecules diffusing in a plane in the presence of a box occupying half of the plane. The borders of the box are impenetrable barriers to the diffusion of the molecules. The pixel size of the simulation is 50 nm. (A) The region measured by a hypothetical camera, with the box shown in red. The yellow contour of the box is copied to panels A, B, C, and D for reference. (B) The diffusion anisotropy map. The anisotropy is large only in the 2 regions corresponding to molecules reaching the barrier (from both sides). (C) Image of the anisotropy angle values obtained in this simulation. Note that the color code represents anisotropy parallel to the wall; for instance, red is horizontal and blue perpendicular. (D) The connectivity map drawn according to the rules explained in the text.

the anisotropy of the pCF polar distribution in the SPRITE (at each point of the image) as the ratio of the long axis to the small axis of the ellipsis representing the SPRITE (see ref 10 for mathematical definition of anisotropy). The values of the anisotropy at each point of the original image are used to produce the diffusion anisotropy map, which is the map of the amount of deformation of the pCF(*R*) at each pixel due to the presence of barriers to diffusion. The concept of a SPRITE should be acquired by the students to be able to continue with the concepts developed in this article. Several examples of SPRITEs can be experimentally built by the students until they grasp the concept.

IV. BARRIER TO DIFFUSION REVEALED BY THE SHAPE OF THE SPRITE

To explain the origin of the deformation of the pCF function caused by a barrier to diffusion, in this article we show with simulations the effect of a barrier on the SPRITE shape. Simulations are performed by the *Simulation* tab in the program SimFCS2 (freely available) or SimFCS4 (Globals Software, G-SOFT Inc., Champaign, IL) and explained in the tutorials that can be found under the *Software* tab on the Laboratory for Fluorescence Dynamics website (14). To show examples of 2D-pCF(τ, *R*), we performed simulations of particles randomly diffusing in a 2D box of 80 $\times$ 80 pixels. A camera is observing only a part of the box (64 $\times$ 64 pixels) to avoid border effects. We placed in the plane of the image a box that represents a barrier to diffusion, as shown in Figure 2A (the box in red). When a molecule is approaching the borders of the box, if the barrier is at a distance less than or equal to the distance used to calculate the pCF(*R*), the amplitude of pCF decreases in the direction of the barrier because the same molecule cannot be observed on the other side of the barrier, as explained in section I. At a relatively large distance from the barrier (on either side of the barrier), the diffusion is isotropic, as determined by the round profile of the SPRITE, and the anisotropy is small. As the SPRITE moves closer to the barrier, though, the round profile becomes deformed in the direction of the barrier; see Figure 1D,E. The same deformation occurs if the molecules are arriving from the other side of the barrier. The net result is that the barrier causes an increase in anisotropy on both sides of the barrier, as shown in Figure 2B.

The direction of the anisotropy is parallel to the border of the obstacle (see Fig 2). On the basis of this observation, we plot the direction of the ellipse representing the SPRITE as a segment of length proportional to the anisotropy. The map of all the segments drawn is called the "connectivity map," which is a convenient way to convey the information of the anisotropy value and the anisotropy direction in a single map (Fig 2D). To avoid filling up the connectivity map with many small segments, we plot a segment only if the anisotropy value is above a given threshold. Both sides of the barrier are clearly visible in the connectivity map, although the barrier is not visible in the intensity image because the

Downloaded from http://meridian.allenpress.com/the-biophysicist/article-pdf/1/2/9/2580574/i2578-6970-1-2-9.pdf by guest on 01 October 2020

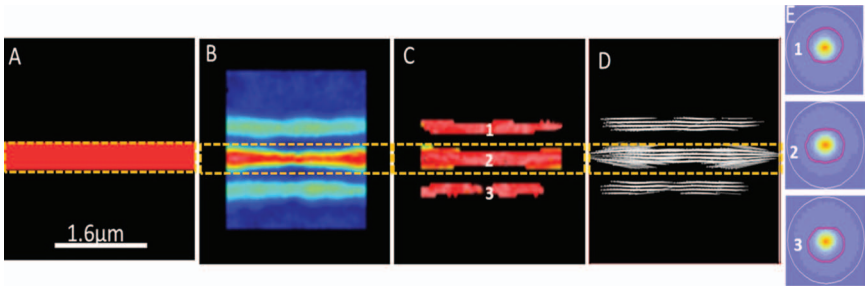

Fig 3. Simulation of fluorescent molecules diffusing in a plane in the presence of a narrow box 8 pixels wide. The borders of the box (indicated by the yellow dots in the figure) are impenetrable barriers to the diffusion of the molecules. The pixel size of the simulation is 0.05 μm. (A) The region measured by a hypothetical camera with the box indicated in red. The yellow contour of the box is copied to all panels for reference. (B) The anisotropy map. The anisotropy is large only in 3 regions corresponding to molecules reaching the barrier from both sides and molecules moving inside the box. (C) The direction of the anisotropy map. Red is 0° and blue is 90°, not found in this simulation. (D) The connectivity map is drawn according to the rules explained in the text. (E) Representative SPRITEs obtained at locations 1, 2, and 3 as indicated in panel C. The SPRITE at 2 is narrow in both sides because of the proximity of the barrier for diffusion at both sides.

molecule density is uniform everywhere in this simulation. The connectivity map can be thought of as a visualization of the molecular flow around obstacles. We will justify the term "connectivity" given to this map with the simulation of the path followed by molecules in narrow channels and in a grid with many channels.

V. SIMULATION OF PARTICLES MOVING IN A PLANE INSIDE A NARROW BOX OF 64 × 8 PIXELS

The borders of the box (the yellow dots in Fig 3A) are an impenetrable barrier for diffusion. If we perform a simulation (with same parameters as used for the previous simulation: 80 particles with uniform density moving randomly with $D = 1\ \mu m^2/s$ and a frame [f] rate of 1000 f/s) but with the presence of a box of narrow width (8 pixels), each of the borders of the box will act as a barrier. Depending on the width of the box (i.e., separation of the barriers), we will see 4 or 3 regions of high anisotropy. However, the deformation is different for the 2D-pCF outside the box (where only one side of the SPRITE is affected) and for points inside the box where both sides of the SPRITE are affected, producing a larger value of anisotropy inside the narrow box (see SPRITEs in Fig 3E, where we show the sequence of SPRITEs calculated for $R = 4$ pixels, with the origin located at different distances from the barrier). This increase in anisotropy is due to the shape of the SPRITE, which is now narrow and extending in only one direction inside the box (Fig 3E, SPRITE at 2). The "connectivity" image shows clearly the narrow path as well as the border of the box (Fig 3D). The anisotropy of the SPRITE increases for molecules moving in narrow channels, as shown in Figure 3B.

VI. SIMULATION OF A CIRCULAR OBSTACLE

In a cell, not all barriers are straight, as assumed for the simulations of Figures 2 and 3. If the curvature of a barrier is small compared with the distance used to calculate the pCF, the flow of molecules close to the barrier will follow a similar behavior as when in the presence of a straight barrier. In this case, the connectivity map is a visual representation of the molecular flow near the barrier. Figure 4 shows the diffusion anisotropy in the presence of a circular box and the resulting connectivity map. As expected from the simulation of straight barriers, the local orientation of the barrier to diffusion is recovered also for this simulation. Note that molecules are present in both sides of the circular barrier, giving the typical anisotropy map with 2 maxima on either side of the barrier (Fig 4B,C). The connectivity map follows the shape of the circular barrier on both the interior and the exterior side of the circular obstacle (Fig 4D).

Downloaded from http://meridian.allenpress.com/the-biophysicist/article-pdf/1/2/9/2580574/i2578-6970-1-2-9.pdf by guest on 01 October 2020

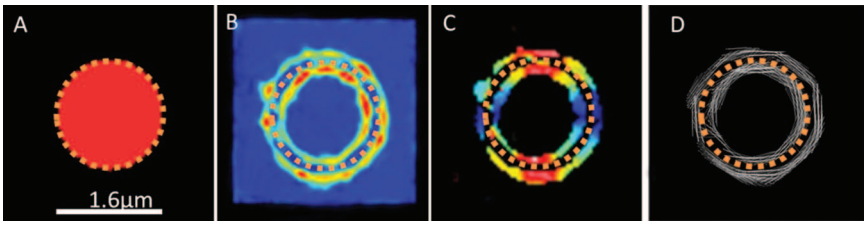

Fig 4. Simulation of fluorescent molecules diffusing in a plane in the presence of a circular obstacle. The borders of the circular obstacle are impenetrable barriers to the diffusion of the molecules. The pixel size of the simulation is 50 nm. (A) The region measured by a hypothetical camera with the box indicated in red. The yellow contour of the circular obstacle is copied to all panels for reference. (B) The diffusion anisotropy map. The anisotropy is large only in 2 circular regions corresponding to molecules reaching the barrier from both sides and molecules moving inside the box. (C) The direction of the anisotropy. Red is 0° and blue is 90°. The direction of the anisotropy changes gradually along the circular obstacle. (D) The connectivity map drawn according to the rules explained in the text. The connectivity map shows the local direction at the border of the circular obstacle. Note that the circular obstacle directs the diffusion of molecules on both sides of the obstacle.

VII. SIMULATION OF AN ARRAY OF SMALL OBSTACLES

What is the minimum size of an obstacle that can be detected? In Figure 5 we show a simulation in which an array of square obstacles of size 8 pixels = 0.4 μm are placed at a center-to-center distance of 16 pixels = 0.8 μm (the pixel size is 0.05 μm). Simulations of diffusion in the presence of obstacles are also available in SimFCS2 or SimFCS4 (14). This situation could represent relatively small obstacles in a cell. If we calculate the pCF at a distance of 4 pixels (200 nm), we should detect motions inside and outside the grid. But at a distance of 7 pixels (350 nm) or larger, the motion inside the grid should not be visible anymore (because the pCF distance is larger than the distance of the barrier from each of the pixels inside the obstacle), and only the path followed by molecules moving between the obstacles should remain visible. This result is shown in Figure 5D. Only the points that are connected outside the grid are shown in the connectivity map. We use the term "connectivity map" to indicate not only the local direction of the obstacles but also the path that molecules follow in a complex structure, such as the simulated array of obstacles.

In this article, using simulations available to students and teachers, we have shown with graphics only that we can follow the trajectories of molecules and that a barrier to diffusion causes a significant perturbation of the SPRITE shape as calculated by the 2D-pCF. The overall motion of molecules in the proximity of obstacles can be visualized with the connectivity map. Because of the limitation of the simulations, we were able to perform simulation only in 2D and in a small field of view (3.2 μm). However, we show that in all cases examined we can visualize the flow of molecules in the proximity and around obstacles.

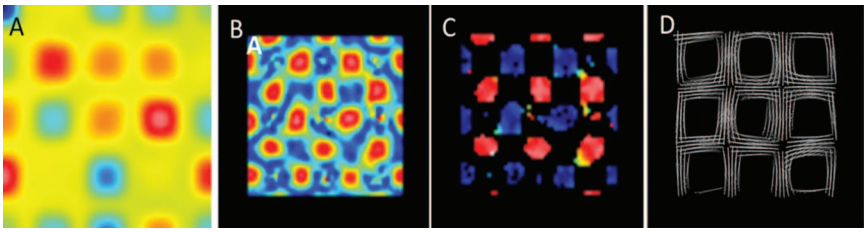

Fig 5. Simulation of molecules moving in a grid. (A) Intensity image of 400-nm obstacles placed at a distance of 800 nm from each other. (B) Anisotropy image calculated at a pair correlation function distance of 7 pixels [pCF(7), 350 nm]. (C) Anisotropy angle image. (D) The connectivity map drawn according to the rules explained in the text. The connectivity map shows the local direction at the border of the grid. Note that the connectivity map displays the grid obstacles by the movement around the obstacles.

Downloaded from http://meridian.allenpress.com/the-biophysicist/article-pdf/1/2/9/2580574/i2578-6970-1-2-9.pdf by guest on 01 October 2020

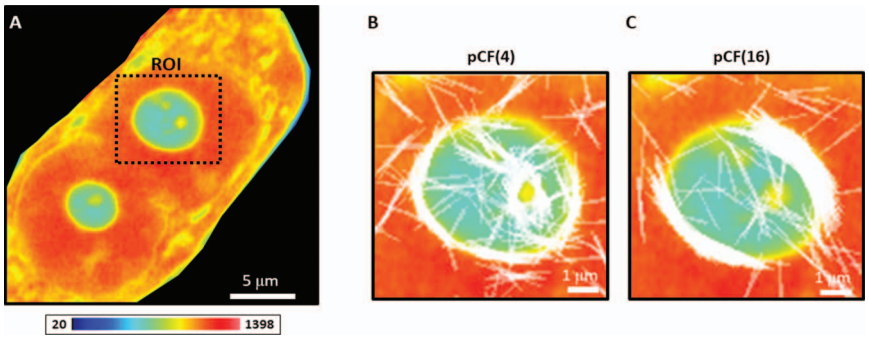

Fig 6. Barriers to diffusion for free enhanced green fluorescent protein (EGFP) in NIH-3T3 cells with the fast-scanner configuration and the Airy detector on the Zeiss LSM 880. (A) Average fluorescence intensity image of NIH-3T3 stable cell line expressing free EGFP. (B) The connectivity map for a pair correlation function at a distance of 4 pixels [pCF(4)] in the indicated ROI, represented as white segments on top of the average intensity image. (C) The connectivity map for a pCF(16) in the indicated ROI.

VIII. MEASUREMENTS OF FLOW ANISOTROPY IN LIVE CELLS AND IN THE CELL NUCLEUS

Single-molecule trajectories show barriers and obstacles to diffusion for enhanced green fluorescent protein in NIH-3T3 cells

Next, we show single-molecule trajectories in cells and identify the existence of barriers to diffusion on the basis of the rules we learned from the simulations. Although in simulations we know what to expect, for the cell interior we do not know where obstacles for diffusion could be. We show the flow of the enhanced green fluorescent protein (EGFP) inside NIH-3T3 cells. EGFP is an inert protein that can diffuse inside cells, thus exploring the intracellular compartment without specific interactions. By using an NIH-3T3 stable cell line expressing EGFP, we found that free EGFP is distributed across the whole cell, but it is partially excluded from the nucleolus, as shown in the fluorescence intensity image in Figure 6A.

The existence of numerous obstacles and barriers for free EGFP inside the cells, in particular in the nucleus, is shown by the 2D-pCF(4) and connectivity maps (Fig 6B,C). In this example, we show the edge of the nucleolus inside the nucleus. These regions can be identified in the fluorescence image of Figure 6A, zoomed in region of interest (ROI). In these images we superimposed the connectivity maps at increasing pCF distances (4 and 16 pixels) on top of the average fluorescence intensity image. The ROI (Fig 6B,C) shows the connectivity around the nucleolus, as well as subnucleolus structures. There is complex connectivity for shorter pCF distance, and the small barriers are disappearing at larger pCF distances (or time). The distances of 4 and 16 pixels show clear evidence for the nucleolus barrier and interestingly subnucleus structures.

IX. DISCUSSION

A. Bleaching and motion artifacts

The basis for the determination of the presence of barriers to diffusion is the deformation of the SPRITE shape. The SPRITE deformation is a differential effect and, in principle, is largely independent of the molecular density, as well as of the average molecular diffusion. Because SPRITE deformation is not dependent on local concentration, the deformation measured by the anisotropy parameter of the SPRITE is largely independent of photobleaching.

B. Effect of the average diffusion coefficient

The deformation of the SPRITE is largely independent of the value of the average diffusion coefficient. Additionally, the SPRITE is plotted on a log-average scale, which makes the shape of the distribution in the SPRITE logarithmically dependent on the value of the diffusion. Of course, the frame rate must be compatible with the rate of motion of the

Downloaded from http://meridian.allenpress.com/the-biophysicist/article-pdf/1/2/9/2580574/i2578-6970-1-2-9.pdf by guest on 01 October 2020

molecules. The pCF shown in Figure 1A can be used to illustrate the effect. The maximum of the pCF(*R*) moves toward shorter correlation times for faster diffusion. However, by increasing the distance *R* in the pCF calculation we can move the peak of the pCF to a longer correlation time. On the contrary, if the diffusion is very slow, we must decrease the camera frame rate to see the broadening of the pCF, which is needed to detect the barrier. The range of diffusion values we tested was from 20 to 0.01 $\mu m^2/s$, which covers most of the diffusion coefficients observed in cells. To show that barriers are still detectable where molecules are diffusing with a small diffusion coefficient, we must compensate by proportionally decreasing the frame rate. This strategy is not always possible, so a very slow moving particle bouncing on a barrier could elude detection.

C. Effect of molecular density

Given a barrier, enough molecules must hit the barrier to deform the SPRITE during the averaging time of the pCF calculation. This condition could require a proper combination of fast diffusion, frame rate, and molecular density. In a few words, we need to have enough events to be able to see a deformation of the SPRITE because of the proximity of a barrier. The consequence is that, for molecules at very low concentration and moving very slowly, we could fail to detect a barrier. Our simulation estimate is that we need the product of the molecule density times the diffusion coefficient to be about (D, $\mu m^2/s$) $\times$ (number of molecules/μm^2), or greater than 2 molecules/s.

D. Raster scan confocal vs. camera

This discussion brings up the question of whether a fast raster scan microscope can be used instead of a camera for collecting data for the detection of barriers to diffusion. Figure 1 shows a simulation of molecules with a diffusion coefficient of 10 $\mu m^2/s$ observed with a camera at 1000 f/s. With the same frame rate, decreasing the particle diffusion to 1 $\mu m^2/s$ still makes the barrier visible with the camera. Decreasing the diffusion further requires increasing the molecule density to detect the existence of the barrier or decreasing the frame rate. The raster scan mode can be beneficial for cases with slow diffusion, even if the collection of many frames can be problematic. The fast scanner module of the new Zeiss LSM 880 or 980 (Carl Zeiss GmbH, Jena, Germany) enables collecting 4 lines at a time, increasing the speed of the acquisition to 10 to 20 ms/f, depending on the image size and number of pixels.

E. Biological relevance of the connectivity information

The presence of barriers and obstacles inside the cell are mandatory to organize and compartmentalize information and processes that need to be separated in time and space. A free diffusing molecule, like EGFP, diffuses inside the cell at 20 to 30 $\mu m^2/s$. EGFP can explore the entire nucleus within a few seconds. Thereby, it is clear that for free diffusing molecules, the occurrence of stable or transitory compartments is needed to organize in time and space the information pipeline. Methods that enable the elucidation of confinement regions are required; however, it should be desirable that these methods could be free of models and fitting that require previous knowledge about the system. The occurrence of transitory barriers, which indeed are thermodynamic barriers due to liquid–liquid phase separation, is gaining more and more attention. However, it is not simple to identify where and when these membraneless organelles will show up. Thereby, this approach will enable us to identify and study these supramolecular organelles without previous assumption and with great spatial and temporal resolution. In particular, fluorescence fluctuation spectroscopy methods are powerful for obtaining valuable information based on the average behavior of single molecules. Instead, the 2D-pCF algorithm provides the unique opportunity to reveal the existence of obstacles and barriers to diffusion based on the deformation of the 2D-pCF without a specific model for the diffusion (10, 11). Here, we apply the method to study a simple biological model.

Downloaded from http://meridian.allenpress.com/the-biophysicist/article-pdf/1/2/9/2580574/i2578-6970-1-2-9.pdf by guest on 01 October 2020

The 2D-pCF method is one of the most sophisticated methods in the family of image correlation spectroscopy, yet it is the only method so far that is capable of informing about the presence of barriers to diffusion in cells and tissues. The method is demanding both conceptually and computationally. In this method, each point of the image is calculated compared with all the surrounding points. If a particle moves in 3D, the correlation function per se is not affected because the particle can return to the plane of the calculation and then be detected again. Other effects, such as the formation of transient holes in structures or membranes, are not specifically discussed in this manuscript (12). Also, the possible effect of erosion of the barrier when molecules interact with the barrier is not discussed. This article is intended to be a guide to explain the concept of 2D-pCF to beginner scientists and to students.

F. Simulations

Simulations were performed by the free SimFCS2 and SimFCS4 software. Random motions of particles in 2D were used for the calculation of the 2D-pCF. From 400 to 800 particles were randomly diffused in a box of 80 $\times$ 80 pixels at different values of the diffusion coefficient, from 20 to 0.01 $\mu m^2/s$. The pixel size for all simulations was 50 nm. In the simulation, a camera is observing only a part of the box (64 $\times$ 64 pixels) at 1000 f/s to avoid border effects. In some simulations when the diffusion coefficient was below 0.1 $\mu m^2/s$, the frame rate of the camera was reduced accordingly. In the plane of the simulation, obstacles defined by a contour line were introduced. In every case, when the particles reached the obstacle, they were not allowed to cross, but all other directions for the random motion were allowed. Simulations lasted for 10 000 frames.

G. Cell culture

NIH-3T3 cells were culture at 37 °C in 5% CO_2 in Dulbecco's modified Eagle's medium (Gibco, Life Technologies, Thermo Fisher Scientific Inc., Huntington Beach, CA) supplemented with 10% fetal bovine serum, with penicillin (100 U/ml) and streptomycin (100 μg/ml). Freshly split cells were plated onto 35-mm MatTek glass-bottom dishes (MatTek Corporation, Ashland, MA) coated with fibronectin (Sigma-Aldrich, St. Louis, MO) 24 h before the experiments. Experiments performed with the Zeiss LSM 880 used the NIH-3T3 stable cell line expressing free EGFP.

X. INSTRUMENTATION

A Zeiss LSM 880 microscope equipped with the Airyscan detector and the fast scanner module was used for the NIH-3T3 cell experiments. A 488-nm Argon laser (Melles Griot, IDEX Health & Science, Rochester, NY) was used for free EGFP excitation and a Zeiss Plan-Apochromat 63×/1.4 Oil DIC M27 objective. Using the fast scanner module and the Airy detector, 4 lines can be acquired simultaneously, achieving a 21 ms/frame time with a 244 $\times$ 244 pixel frame size and a pixel size of 100 nm. The microscope is equipped with temperature and CO_2 controls set up at 37 °C for the experiments.

XI. DATA ANALYSIS AND PROCESSING

All data was analyzed by SimFCS software (G-SOFT Inc.). A detailed tutorial for the 2D-pCF processing and analysis can be found at the LFD web page (14). A free edition of the software called SimFCS2 is also available at our website and SimFCS4 will become freely available after June 2020.

XII. DATA AVAILABILITY

All data are available at the LFD web site (14).

ACKNOWLEDGMENTS

We thank Christoph Gohlke for developing the fast routines for the calculation of the 2D-pCF sprites method. This work was supported in part by grants NIH P41-GM103540 and NIH P50-GM076516. LM is in part supported by the Universidad de la República-Uruguay as a full time professor.

AUTHOR CONTRIBUTIONS

LM and PNH carried out all of the imaging and data analysis and prepared the manuscript. BT prepared the stable cell lines and carried out the imaging on the Zeiss LSM 880 and analyzed

Downloaded from http://meridian.allenpress.com/the-biophysicist/article-pdf/1/2/9/2580574/i2578-6970-1-2-9.pdf by guest on 01 October 2020

the data. EG, LM, and PNH conceived the project. EG prepared and performed all simulations and reviewed the manuscript. EG, LM, and PNH wrote and corrected the manuscript.

REFERENCES

1. Di Rienzo, C., V. Piazza, E. Gratton, F. Beltram, and F. Cardarelli. 2014. Probing short-range protein Brownian motion in the cytoplasm of living cells. *Nat Commun* 5:5891.
2. Di Rienzo, C., F. Cardarelli, M. Di Luca, F. Beltram, and E. Gratton. 2016. Diffusion tensor analysis by two-dimensional pair correlation of fluorescence fluctuations in cells. *Biophys J* 111:841–851.
3. Cardarelli, F., L. Lanzano, and E. Gratton. 2011. Fluorescence correlation spectroscopy of intact nuclear pore complexes. *Biophys J* 101:L27–L29.
4. Hyman, A. A., and K. Simons. 2012. Cell biology. Beyond oil and water—phase transitions in cells. *Science* 337:1047–1049.
5. Brangwynne, C. P. 2013. Phase transitions and size scaling of membrane-less organelles. *J Cell Biol* 203:875–881.
6. Zhu, L., and C. P. Brangwynne. 2015. Nuclear bodies: the emerging biophysics of nucleoplasmic phases. *Curr Opin Cell Biol* 34:23–30.
7. Kusumi, A., Y. Sako, and M. Yamamoto. 1993. Confined lateral diffusion of membrane receptors as studied by single particle tracking (nanovid microscopy). Effects of calcium-induced differentiation in cultured epithelial cells. *Biophys J* 65:2021–2040.
8. Hebert, B., S. Costantino, and P. W. Wiseman. 2005. Spatiotemporal image correlation spectroscopy (STICS) theory, verification, and application to protein velocity mapping in living CHO cells. *Biophys J* 88:3601–3614.
9. Jacobson, K., Z. Derzko, E. S. Wu, Y. Hou, and G. Poste. 1976. Measurement of the lateral mobility of cell surface components in single, living cells by fluorescence recovery after photobleaching. *J Supramol Struct* 5:565(417)–576(428).
10. Malacrida, L., P. N. Hedde, S. Ranjit, F. Cardarelli, and E. Gratton. 2018. Visualization of barriers and obstacles to molecular diffusion in live cells by spatial pair-cross-correlation in two dimensions. *Biomed Opt Express* 9:303–321.
11. Malacrida, L., E. Rao, and E. Gratton. 2018. Comparison between iMSD and 2D-pCF analysis for molecular motion studies on in vivo cells: the case of the epidermal growth factor receptor. *Methods* 140–141:74–84.
12. Magde, D., E. Elson, and W. W. Webb. 1972. Thermodynamic fluctuations in a reacting system—measurement by fluorescence correlation spectroscopy. *Phys Rev Lett* 29(11):705–708.
13. Jameson, David M. 2014. Introduction to Fluorescence. CRC Press, Boca Raton, FL.
14. Laboratory for Fluorescence Dynamics. 2020. Accessed 22 June 2020. https://www.lfd.uci.edu/globals.
15. Pozzi, D., C. Marchini, F. Cardarelli, F. Salomone, S. Coppola, M. Montani, M. E. Zabaleta, M. A. Digman, E. Gratton, V. Colapicchioni, and G. Caracciolo. 2014. Mechanistic evaluation of the transfection barriers involved in lipid-mediated gene delivery: interplay between nanostructure and composition. *Biochim Biophys Acta* 1838:957–967.

Downloaded from http://meridian.allenpress.com/the-biophysicist/article-pdf/1/2/9/2580574/i2578-6970-1-2-9.pdf by guest on 01 October 2020